

# The effect of fabrication conditions on optical characteristics of CQDs prepared by micro plasma

Pham Van Duong, Do Hoang Tung, Pham Hong Minh,  
Doan Thi Kieu Anh, Nguyen Thanh Binh\*

*Institute of Physics, Vietnam Academy of Science and Technology,  
No. 10 Dao Tan, Giang Vo, Ha Noi, Viet Nam*

\*Email: [tbnguyen@iop.vast.vn](mailto:tbnguyen@iop.vast.vn)

Received: 17 January 2023; Accepted for publication: 8 May 2023

**Abstract.** Carbon quantum dots (CQDs) are emerging nanomaterials with outstanding advantages such as non-toxicity, high biocompatibility, and abundant functional groups, making them highly suitable for biological and optoelectronic applications. In this study, CQDs were synthesized using a solution-interaction microplasma method operated at atmospheric pressure. The obtained CQDs exhibit spherical morphology with particle sizes below 10 nm and demonstrate excitation-dependent fluorescence over the 350 - 650 nm wavelength range. The effects of fabrication parameters-including plasma electrode polarization, precursor concentration, and preparation time-on the optical properties of CQDs were systematically investigated. Variations in these conditions resulted in changes in fluorescence intensity, spectral width, and emission peak position, reflecting the strong dependence of optical behavior on surface states and structural features. The results confirm that microplasma synthesis enables effective tuning of CQD optical properties, providing insights into exciton self-trapped emission (EST) and supporting the development of environmentally friendly CQD-based fluorescent materials for potential display and sensing applications.

**Keywords:** Nano carbon quantum dots, solution-interaction microplasma method.

**Classification numbers:** 2.1.1, 2.4.4, 2.5.3, 2.10.2.

## 1. INTRODUCTION

Carbon nano quantum dots or carbon quantum dots (CQDs) were discovered by Xu *et al.* during the refining process of carbon nanotubes. This is a new member of the family of semiconductor quantum dot-like luminescent nanomaterials [1 - 4]. The luminescence properties of CQDs can be applied in many fields such as imaging/biosensors, photocatalysis, and optoelectronic device components [4, 5]. Compared with commonly used metal-semiconductor-based quantum dots, CQDs have high chemical stability, good solubility in water, high biocompatibility, and lower toxicity. CQDs indicating the huge potential for applications in the field of biological applications, including bioimaging, drug delivery, and cancer therapy [6].

There are several methods used for CQDs, and the choice of method depends on the desired properties and application of the dots. Fabrication methods of CQDs fall into two categories: top-down and bottom-up routes [4 - 6]. The top-down routes involve breaking down large-size graphene, CNTs, carbon nanofibers or other bulk carbon materials into CDs; while bottom-up routes are achieved by polymerization and carbonization of small molecules or polymers as precursors. Both top-down and bottom-up routes can be fulfilled by chemical oxidation, laser ablation approach, electrochemical synthesis, hydrothermal/solvothermal synthesis, pyrolysis reaction and microwave treatment. One common method is the hydrothermal method, which involves heating a carbon source, such as citric acid, in the presence of a stabilizing agent, such as polyethylene glycol, under high-pressure conditions. This method produces carbon dots with good water solubility and size control [7]. Another method is microwave-assisted synthesis, which involves heating the carbon source in a microwave reactor to produce carbon dots with high fluorescence and a narrow size distribution [8]. Additionally, laser ablation, electrochemical oxidation, and photochemical methods are also commonly used to fabricate carbon dots [9]. Each method offers unique advantages and disadvantages in terms of size distribution, fluorescence intensity, and stability. However, these synthesis methods of CQDs all face challenges such as using initial toxic materials, requiring special reaction conditions, complex synthesis processes, and low quantum efficiency. Some methods require synthesis at high temperatures, which speeds up the chemical reaction but also leads to the creation of undesirable by-products. The solution-interaction microplasma method is a promising method for widely applied materials synthesis, catalyst treatment and nanomaterial synthesis. This method is performed at room temperature and used initially environmentally friendly precursors, but a few by-products might still appear [10]. The nanoparticle size can be adjusted by changing the discharge time and voltage between the electrodes. In addition, free radicals, such as  $\cdot\text{OH}$ ,  $\cdot\text{O}^2$ ,  $\cdot\text{H}^+$ ,  $\text{N}^+$ , can be formed from the solution via solution-interaction microplasma. This feature enables the incorporation of surface functions of CQDs without the use of additional solvents.

In this report, we present the results of the fabrication of carbon quantum dots by the solution-interaction microplasma method. Besides, the influence of fabrication conditions on optical characteristics of quantum dots, including electrode change, fabrication time, precursor solution concentration, and electrolyte concentration in solution was evaluated.

## 2. MATERIALS AND METHODS

Figure 1 shows a schematic diagram of the microplasma system for making carbon nanoscale quantum dots by the solution-interaction plasma method. The microplasma system for the synthesis of CQDs includes a high-voltage DC 5900 V power source, a plasma injector, and two electrodes: a working electrode for creating plasma (plasma electrode) and a grounding electrode; a cup of 50 ml (Bomex) contains 20 ml of the precursor solution. Argon gas is blown into the plasma injector, which is a hollow glass tube with an outer diameter of 15 mm and an inner diameter of 10 mm. The injector covers a plasma electrode and has an argon gas flow rate of 100 sccm. The Molybdenum (Mo) plasma electrode is placed 0.75 cm away from the surface of the precursor solution and connected to a 100 k $\Omega$  capacity resistor. The gold (Au) ground electrode is immersed in a precursor solution. The DC potential applied to the plasma electrode can change as a negative or positive potential relative to the earth electrode.

The precursor solution used to synthesize CQDs is a mixture of sucrose solution ( $\text{C}_{12}\text{H}_{22}\text{O}_{11}$ , Guangdong Guanghua Sci-Tech Co., Ltd, China) with a variable content (12.5 - 200 g/l) in an aqueous solution of NaOH (0.25 - 4 g/ml  $\text{H}_2\text{O}$ , Xilong Scientific Co., Ltd., China),

whose rate varies depending on experimental conditions. The plasma-generating current was maintained constant throughout the sample preparation at 5 mA. The temperature of the solution in contact with the plasma changes between 30 °C and 40 °C after 30 minutes of fabrication.

The synthesis and mechanism study of these reactants has also been explored using other synthesis methods [10 - 12]. Sucrose is used as a carbon source to make carbon quantum dots, which form through the dehydration and polymerization

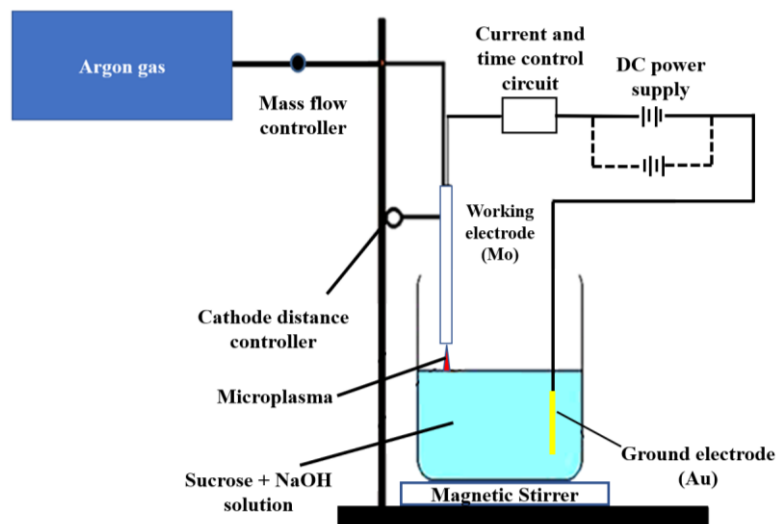


Figure 1. Schematic of microplasma system for fabricated carbon quantum dots.

of NaOH and  $C_{12}H_{22}O_{11}$  with the assistance of plasma energy, as shown in Figure 2.

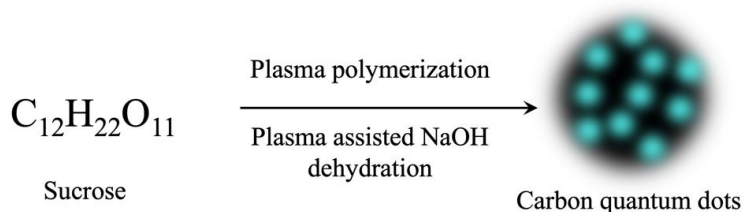


Figure 2. Mechanism of formation of CQDs by micro plasma.

The samples after fabrication were examined for their structural morphology by Transmission electron microscopy (TEM), high resolution scanning electron microscope (SEM- Regulus 8100 Hitachi, Japan), Fourier transform infrared spectroscopy (Cary FTIR 630 Agilent), and optical properties were investigated on the UV-Vis-Nir UV2600 spectroscopy system (Shimadzu); Cary Eclipse fluorescence spectrometer (Agilent).

### 3. RESULTS AND DISCUSSION

#### 3.1. Morphological and structural characteristics of carbon nano-quantum dots

The results of SEM, TEM imaging, and infrared absorption spectroscopy show no significant differences in the structural morphology of the fabricated CQDs under various

conditions, such as synthesis time, precursor concentration, and polarized voltage. Figure 3 shows TEM and SEM image of CQDs fabricated from NaOH 1 g/l; Sucrose: 100 g/l in 30 minutes with the positive applied voltage.

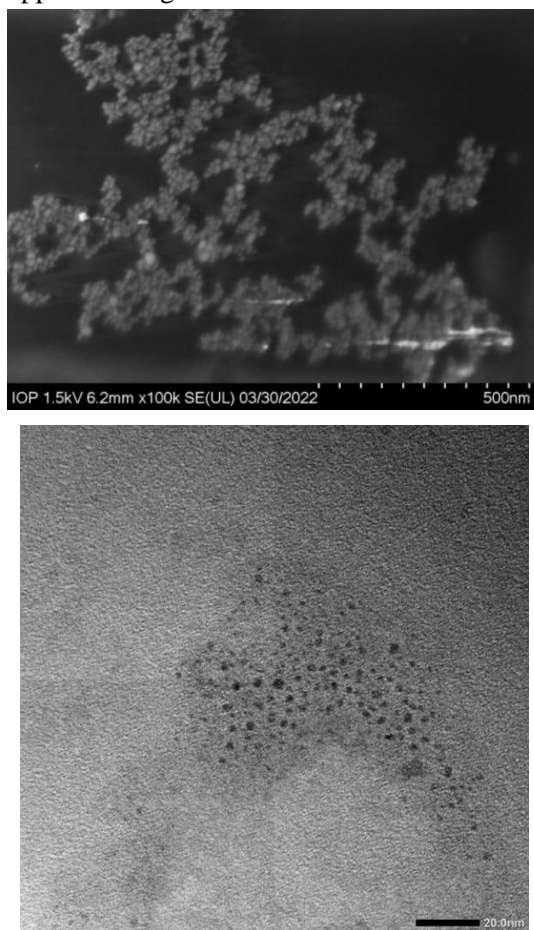


*Figure 3. SEM and TEM image of CQDs prepared from NaOH 1 g/l; Sucrose: 100g/l in 30 minutes with the positive applied voltage.*

The TEM and SEM images show that CQDs have a spherical or quasi-spherical shape, with particle sizes less than 10 nm. The particles are arranged in clusters, they form a layer on the substrate plane. This clustering of particles can be explained by the surface tension of the solvent, which is generated by evaporation. In liquid solvents, the CQDs exist in suspension, which is not deposited after fabrication. The particle size and average size distribution of CQDs from TEM images were also previously reported, which were used with the same method and precursor concentration for fabrication [13].

Figure 4 shows the FTIR infrared absorption spectrum of the fabricated carbon quantum dot. In the observed spectrum, absorption peaks at  $3260\text{ cm}^{-1}$ ,  $2100\text{ cm}^{-1}$ ,  $1620\text{ cm}^{-1}$ , and  $1036\text{ cm}^{-1}$  correspond to the vibrations of the bonds  $\text{-OH}$ ,  $\text{C}\equiv\text{C}$ ,  $\text{H-O-H}$ ,  $\text{C=O}$ ,  $\text{C=C}$ , and  $\text{-CH}_2$  correspondingly [8]. These associations derive from CQDs or functional groups of CQDs. The positions and intensities of the infrared absorption peaks remain virtually unchanged for the fabricated samples under different conditions. Interestingly, this is indicated in fluorescence

properties and confirms that the fabricated CQDs have rich functional groups suitable for doping many different pigments for each specific application.

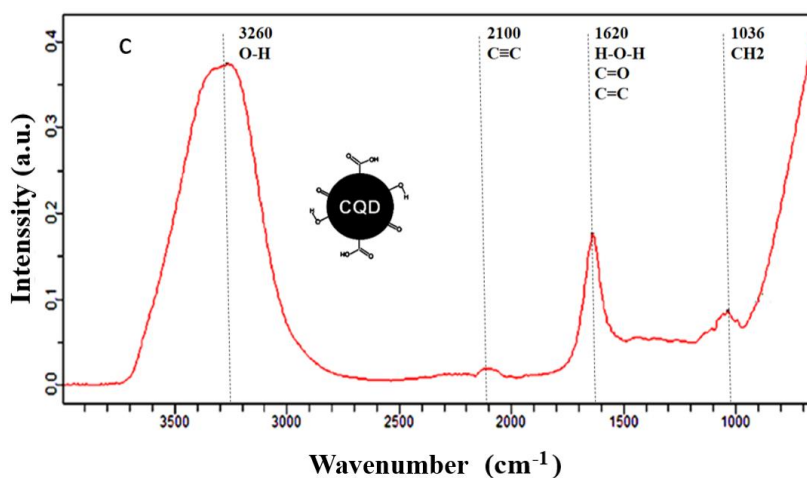


Figure 4. FTIR infrared absorption spectra of the fabricated CQDs.

### 3.2. Carbon quantum dot optical properties

The absorption and stationary emission spectra of CQDs observed using a Shimadzu UV-Vis UV-2600 absorption spectrometer and a Cary Eclipse fluorescence instrument are shown in Figure 5a. There are no significant differences in the shape and position of the absorption spectrum of the CQDs samples prepared under different conditions. CQDs exhibit strong absorption in the ultraviolet wavelength domain, with the tail extending into the visible region. This absorption is caused by electrons transitioning from the orbital to C=N bonds, as well as electronic transitions from C–O [14] and the  $\pi$ - $\pi^*$  transition of C=C [15].

The optical absorption of carbon nanoscale quantum dots can be converted to longer wavelengths by surface passivation and doping with a suitable doping agent. Furthermore, the functional groups on the surface of CQDs also play an important role in their absorption properties. Absorption of CQDs occurs at wavelengths below 550 nm and gradually increases towards short wavelengths, with double absorption at 400 nm and 350 nm. The fluorescence spectra show that the carbon nanoparticle quantum dots exhibit optical properties that are dependent on the excitation wavelength in the range of 350 - 650 nm.

Figure 5a-b shows the emission spectra as a function of excitation wavelengths, Figure 5c displays the normalized intensity of the fluorescence. Emission spectra of the CQDs can be observed at excitation wavelengths from 320 nm. However, at excitation wavelengths below 380 nm, the peak position of the fluorescence spectrum remains relatively constant, the fluorescence intensity is weak, and the obtained spectrum is diffracted compared to measurements made at other excitation wavelengths. On the other hand, a clear fluorescence peak shift is observed as a function of excitation wavelength increases above 380 nm, while the fluorescence intensity decreases gradually and the spectral width increases. The obtained fluorescence spectra are smooth and stable compared to those obtained at excitation wavelengths below 380 nm. At excitation wavelengths above 520 nm, the fluorescence signal is still present. However, the sharp increase in spectral width makes it difficult to observe the peak, as its position is located next to the excitation wavelength. Figure 5d depicts the dependence of the fluorescence peak of

CQDs on the excitation wavelength, and it shows a linear relationship between the fluorescence peak and the excitation wavelength.

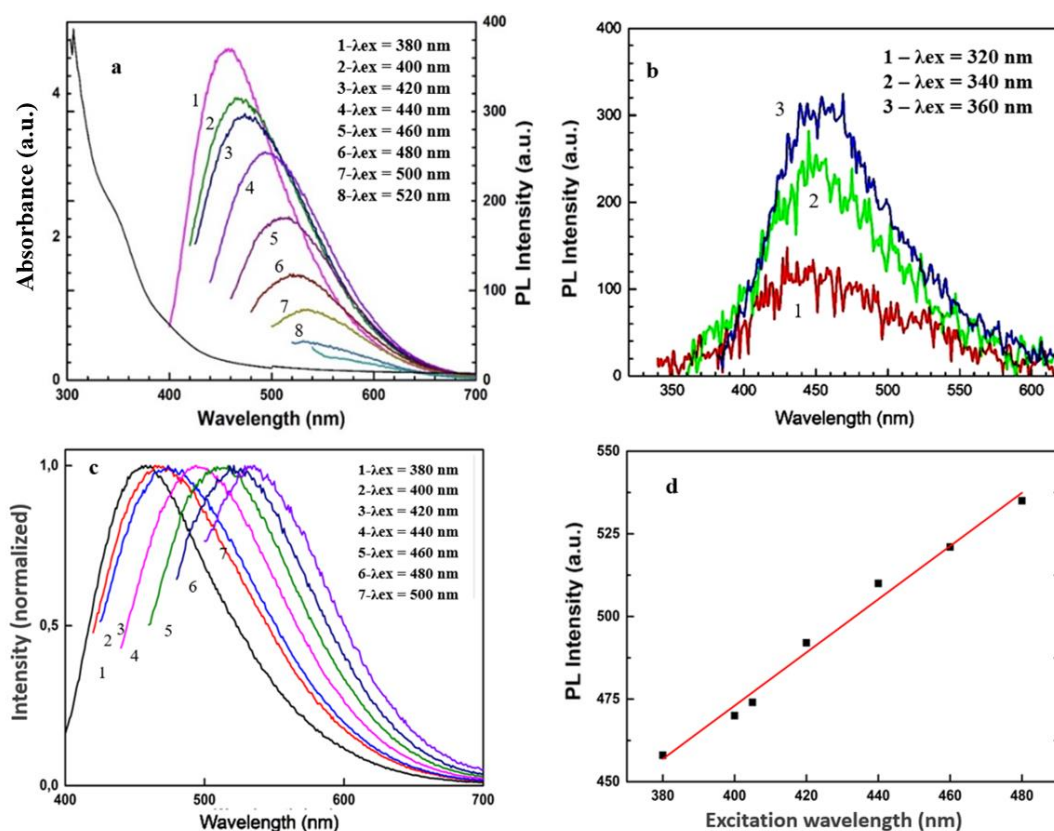


Figure 5. The absorption spectra of CQDs were obtained from a precursor solution of 20 ml with sucrose concentration of 100 g/l and NaOH concentration of 1 g/l, prepared for 30 minutes (5a). The emission spectra as a function of excitation wavelengths (5a-5c), and a linear dependence of fluorescence intensity on excitation wavelength (5d).

### 3.3. The effect of manufacturing conditions on the luminescence properties of CQDs

The fluorescence spectra of CQDs fabricated at positive or negative plasma polarization potential and the concentration of NaOH and sucrose in the precursor solution did not have much change in spectral form, as shown in Figure 6a. It can be seen that there is no difference change in the position of the fluorescence peak when the fluorescence spectra of CQDs fabricated with the concentration of 1 g/l NaOH precursor and 100 g/l sucrose, using negative and positive potentials applied to the plasma electrode (Figure 6a). However, the fluorescence spectral width of CQDs with the negative potential direction has a small change compared to the sample prepared with the positive potential direction, and the fluorescence peak intensity is also larger. The change in fluorescence properties of CQDs with the same precursor concentration but changed plasma polarization potential is due to the reaction of forming CQDs when the plasma polarization potential is negative and positive, leading to quality CQDs, the functional groups formed in addition to different CQDs. The electronic interaction mechanism causing the difference in input voltage on the fluorescence spectra of CQDs is still being studied.



The influence of fabrication conditions such as precursor concentration (sucrose, NaOH), fabrication time and electrode orientation on the photodynamic characteristics of CQDs were investigated. Figure 6b shows the change of concentration of precursor solution with sucrose content (12.5 - 200 g/l) and constant concentration of NaOH electrolyte 1 g/l prepared in 30 minutes with positive voltage direction. Figure 6c shows the dependence of the fluorescence spectrum with the NaOH electrolyte concentration varying from 0.25 g/l to 4 g/l when the sugar concentration is 100 g/l and the fabrication time is 30 minutes. Figure 6d presents the change of fluorescence spectra of CQDs with the time of sample preparation with the concentration of precursor solution (sucrose 100 g/l, NaOH 1 g/l) constant. The samples were excited at 405 nm for comparison in terms of fluorescence spectral intensities.

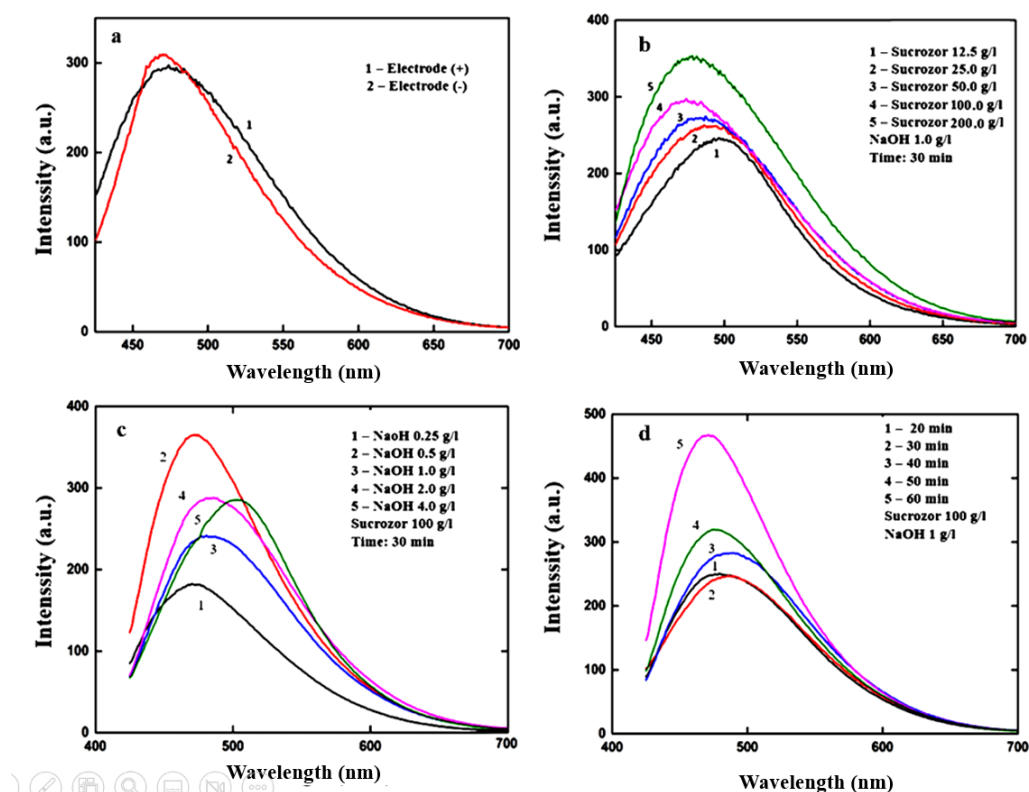


Figure 6. The fluorescence spectra of CQDs were fabricated with a) different electrodes, b) precursor solution concentration, c) electrolyte concentration and d) different fabrication times, when excited by 405 nm.

In Figures 6b-d, the fluorescence spectroscopy results show that the fluorescence intensity of CQDs and spectral width gradually increase as the precursor concentration and fabrication time are increased. When the fabrication conditions are increased to a certain threshold, the fluorescence intensity gradually decreases and there is a shift of the peak of the spectrum towards the longer wavelength.

This effect has been found in most of the nanocarbon nanostructured materials and shown in previous publications [15, 16], the dependence of the fluorescence intensity on the excitation wavelength for CQDs is mainly derived from the heterogeneous surface state, size and electronic properties of heteroatoms. For the case of CQDs with multiple surface functional groups, the

presence of surface states can change the band gap and radiant energy state of the CQDs. Under optical excitation, electrons are promoted to higher energy states in the conduction band, that are far away from the radiating electronic states caused by the surface effect. Therefore, the ability to emit photons from CQDs is reduced as the concentration of carbon quantum dots increases. This is a consequence of the fluorescence emission from CQDs with unevenly distributed functional groups affecting the radiative recombination of electron-hole pairs formed by the  $sp^2$  conjugated domain and neighboring state groups [17, 18]. The emission mechanism proposed here is: (i) the emission of CQDs electrons is achieved through the  $\pi-\pi^*$  conversion from the  $sp^2$  conjugated domain to the  $n-\pi^*$  transition, (ii) the atom is recovered from the  $n-\pi^*$  state to the C=O energy level through a nonradiative transition, and (iii) radiative recombination for holes in the  $sp^2$  state to neighboring states [19]. The approach is discrete since electrons are produced by different functional groups [20].

#### 4. CONCLUSION

We employed a simple, fast, and environmentally friendly method to synthesize carbon quantum dots (CQDs) that have abundant functional groups and a particle size of less than 10 nm. CQDs also have a wide fluorescence emission spectral region from 350 to 650 nm, and the peak of the emission spectrum changes with the excitation wavelength. However, preparation conditions such as the polarization potential applied to the plasma electrode, precursor concentration, and preparation time can affect the optical properties of CQDs. CQDs made with negative polarization potential have a narrower spectral width and higher intensity than those made with positive polarization potential, possibly due to the formation of CQDs and different functional groups. The fluorescence intensity and emission peak of CQDs shift with changes in precursor concentration and fabrication time. The cause of the change in optical properties of CQDs will be studied more closely in the following works.

**Acknowledgments.** This research was funded by the project under the Physics Program at the Vietnam Academy of Science and Technology (Project No. KHCBVL.05/21-22), Project No. QTBY01.04/20-21 and the International Center of Physics (through project number ICP.2022.11).

**CRedit authorship contribution statement.** P.V. Duong, D. T. K. Anh conceived the experiment. P.V.Duong, D. H. Tung conducted the experiments and analyzed the data. All authors participated in the discussion of the results; P. V. Duong, D. H. Tung, P. H. Minh and N. T. Binh. P. V. Duong wrote the initial draft of the paper. N. T. Binh and P. V. Duong supervised the project. All authors have read and agreed to the published version of the manuscript.

**Declaration of competing interest.** The authors declare that they have no competing financial interests.

#### REFERENCES

1. Hao S. L., Il J., Rong X., Seungju S., Jin-Wook L., Chao L., Amrita P., Sergei M., Mark S. G., Yang Y., Shigeo M., Yutaka M. - Achieving high efficiency in solution-processed perovskite solar cells using  $C_{60}/C_{70}$  mixed fullerenes, *ACS Appl. Mater. Interfaces* **10** (2018) 39590-39598. doi.org/10.1021/acsami.8b11049.
2. Adam J. C., Mustafa K. B., Stephen A. H., Neal T. S., Christopher A. H., and Milo S. P. S. - Charged carbon nanomaterials: Redox chemistries of fullerenes, carbon nanotubes, and graphenes. *Chem. Rev.* **118** (2018) 7363-7408. doi.org/10.1021/acs.chemrev.8b00128.



3. Vasilios G., Jason A. P., Jiri T., Radek Z. - Broad family of carbon nanoallotropes: Classification, chemistry, and applications of fullerenes, carbon dots, nanotubes, graphene, nanodiamonds, and combined superstructures. *Chem. Rev.* **115** (2015) 4744-4822. doi.org/10.1021/cr500304f.
4. Xiaoyou X., Robert R., Yunlong G., Harry J. P., Latha G., Kyle R. and Walter A. S. - Electrophoretic analysis and purification of fluorescent single-walled carbon nanotube fragments. *Chem. Soc.* **126** (2004) 12736-12737. doi.org/10.1021/ja040082h.
5. Xunzhi H., Yongsheng L., Xiaoxia Z., Amanda E. R., Kostya (Ken) O. - Fast microplasma synthesis of blue luminescent carbon quantum dots at ambient conditions. *Plasma Process. Polym.* **12** (2015) 59-65. doi.org/10.1002/ppap.201400133.
6. Chuang H., Peng X., Xuanhan Z., Wujian L. - The synthetic strategies, photoluminescence mechanisms and promising applications of carbon dots: Current state and future perspective. *Carbon* **186** (2022) 91-127. doi.org/10.1016/j.carbon.2021.10.002.
7. J. Zheng, Y. Wang, F. Zhang, Y. Yang, X. Liu, K. Guo, H. Wang, B. Xu. - Microwave-assisted hydrothermal synthesis of solid-state carbon dots with intensive emission for white light-emitting devices. *J. Mater. Chem. C* **32** (2017) 8105-8111. doi.org/10.1039/C7TC01701D.
8. Chong Q., Huaidong W., Ailing Y., Xiaoxu W. and Jie X. - Facile fabrication of highly fluorescent n-doped carbon quantum dots using an ultrasonic-assisted hydrothermal method: optical properties and cell imaging. *ACS Omega* **6** (2021) 32904-32916. doi.org/10.1021/acsomega.1c04903.
9. Y. P. Sun, B. Zhou, Y. Lin, W. Wang, K. A. S. Fernando, P. Pathak, M. J. Mezziani, B. A. Harruff, X. Wang, H. Wang, P.G. Luo, H. Yang, M. E. Kose, B. Chen, L.M. Veca, S. Y. Xie. - Quantum-sized carbon dots for bright and colorful photoluminescence, *J. Am. Chem. Soc.* **24** (2006) 7756-7757. doi: 10.1021/ja062677d.
10. Y. Li, X. Zhong, A. E. Rider, S. A. Furman, K. Ostrikov. - Fast, energy-efficient synthesis of luminescent carbon quantum dots, *Green Chem.* **16**(5) (2014) 2566-2570. doi: 10.1039/c3gc42562b.
11. Athanasios B. B., Georgios T., Michael A. K., Maria B., Antonios K., Dimitrios G., Aristides B., Katerina H., Ondrej K., Radek Z., Irene P., Panagiotis A., Stelios C. - Green and simple route toward boron doped carbon dots with significantly enhanced non-linear optical properties, *Carbon* **83** (2015) 173-179. doi.org/10.1016/j.carbon.2014.11.032
12. R. Y. Li, X. Wang, Z. J. Li, H. Y. Zhu, J. K. Li. - Folic acid-functionalized graphene quantum dots with tunable fluorescence emission for cancer cell imaging and optical detection of Hg<sup>2+</sup>, *New J. Chem.* **42** (2018) 4352–4360. doi.org/10.1039/C7NJ05052F.
13. Do H. T., Tran T. T., Nguyen D. C., Nguyen T. L., Nguyen V. K., Le H. M., Pham H. M., Nguyen T. T. T., Nguyen M. H., Nguyen V. P. - Facile synthesis of carbon quantum dots by plasma-liquid interaction method, *Communications in Physics* **27** (2017) 311-316. doi.org/10.15625/0868-3166/27/4/10867.
14. Lin L. X., Zhang S. W. - Creating high yield water soluble luminescent graphene quantum dots via exfoliating and disintegrating carbon nanotubes and graphite flakes. *Chem. Commun.* **48** (2012) 10177-10179. doi.org/10.1039/C2CC35559K.
15. Vikas K. S., Virendra S., Pradeep K. Y., Subhash C., Daraksha B., Vijay K., Biplob K., Mahe T. and Syed H. H. - Bright-blue-emission nitrogen and phosphorus doped carbon quantum dots as a promising nanoprobe for detection of Cr(VI) and ascorbic acid in pure

- aqueous solution and in living cell. *New J. Chem.* **42** (2018) 12990-12997. doi.org/10.1039/C8NJ02126K.
16. Ju T., Jin Z., Yunfei Z., Yiming X., Yanli S., Yunhua C., Lan D., Wen X. - Influence of group modification at the edges of carbon quantum dots on fluorescent emission. *Nanoscale Research Letters* **14** (2019) 241. doi.org/10.1186/s11671-019-3079-7.
  17. Fanglong Y., Ting Y., Laizhi S., Zhibin W., Zifan X., Yunchao L., Xiaohong L., Louzhen F., Zhan'ao T., Anmin C., Mingxing J., Shihe Y. - Engineering triangular carbon quantum dots with unprecedented narrow bandwidth emission for multicolored LEDs. *Nature Communications* **9** (2018) 2249. doi: 10.1038/s41467-018-04635-5.
  18. Shoujun Z., Yubin S., Xiaohuan Z., Jieren S., Junhu Z., Bai Y. - The photoluminescence mechanism in carbon dots (graphene quantum dots, carbon nanodots, and polymer dots): current state and future perspective. *Nano Research* **8** (2015) 375-381. doi.org/10.1007/s12274-014-0644-3.
  19. P. V. Duong, N. M. Hoa, L. D. Toan, P. T. Chuyen, N. T. T. Hien, P. H. Minh, N. T. Binh and L. A. Thi. - Plasma-assisted green fabrication of fluorescent carbon quantum dot-silver nanocomposites. *Journal of Dispersion Science and Technology* **46** (2025) 1356-1364. <https://doi.org/10.1080/01932691.2024.2440422>
  20. P. V. Duong, L. A. Thi, L. D. Toan, P. H. Minh, N.T. Binh, D. H. Tung, N. D. Lam and N. M. Hoa. - Size-Dependent Optical Properties and Exciton Self Trapping Emission in Carbon Quantum Dots. *ChemistrySelect* **9** (2024) e202401754 (1 of 7). doi.org/10.1002/slct.202401754.